Sizing up protoplanetary disks

Trapman, L.

1 Introduction

If there is one thing we can be certain about, it is that planets can be formed. The evidence for that is literally beneath our feet. However, knowing that it can happen and understanding how are two completely different things. The search for understanding planet formation started out focused on our Solar System, arguably with the advent of astronomy itself, but after the discovery of exoplanets orbiting other stars (Mayor & Queloz 1995) has since expanded considerably. The total number of exoplanets found currently stands at 4348[1], a number that will be outdated by the time you read this thesis. Exoplanets are found in a large variety of planetary systems, from multiple terrestrial planets packed inside the central $\sim 0.3-1$ AU (e.g., TRAPPIST-1 or Kepler-90, Gillon et al. 2017; Cabrera et al. 2014) to several gas giants spread over ~ 70 AU from the central star (e.g., HR 8799, Marois et al. 2010). The origins of these planetary systems lie in disks of gas and dust that surround young stars while they are being formed. The diverse outcomes of planet formation are intimately linked to these *protoplanetary disks* in which planets form and grow. How much material do disks contain for planet formation? And is this material concentrated close to the star or spread out over a large area? Answering these questions will help us solve the riddle of planet formation.

1.1 From clouds to cores to disks

To be able to discuss under which conditions planets are formed we first have to zoom out to before that process starts, to the giant molecular clouds in which stars form. As the name suggests, these clouds are made up of molecular gas that consists of H_2, CO, N_2 and He. In addition to their gaseous component these molecular clouds also contain small dust grains, with sizes up to 1μm, that make up about one percent of the total mass of the cloud (e.g. Draine 2003). The clouds were first identified and characterized using the background stars they obscured (see, e.g. Barnard 1919; Bok 1948; Cambrésy 1999). At longer wavelengths these clouds become translucent. Observations at far-infrared wavelengths used the blackbody radiation of dust grains of these clouds to study their filamentary internal structure in detail (see, e.g. André et al. 2010; Miville-Deschênes et al. 2010; Ward-Thompson et al. 2010).

The origin of filaments in clouds are still debated, with both turbulence (see, e.g. McKee & Ostriker 2007; Hill et al. 2011; Tafalla & Hacar 2015) and magnetic fields (see, e.g. Nakamura & Li 2008; Peretto et al. 2012; Palmeirim et al. 2013) being proposed

[1] `http://www.exoplanet.eu`, as of 24 September 2020

to play a role in their formation. Inside these filaments one can find so-called dense cores, overdensities $\sim 0.01 - 0.1$ parsec in size with a mass between 0.01 and 10 $M_\odot$ that are bound by their own gravity (see, e.g. Bontemps et al. 2010; Könyves et al. 2010; Maury et al. 2011). Internal forces resulting from turbulence and magnetic fields are able to partially balance the inward gravitational force, but eventually gravity will win out and the core will start to collapse, forming one up to a few stars at its center.

When a several 1000 AU size core collapses it contains too much angular momentum for all of the material to be accreted directly onto the forming protostar that is at most a few solar radii across: the rotational speed required would break up the star (see, e.g. Goodman et al. 1993). Some of the angular momentum can be dissipated by magnetic breaking (see e.g. Li et al. 2014) or can go in the orbital angular momentum of a binary in the case where multiple stars form (see, e.g. Reipurth et al. 2014), but observations show that in most cases there is some angular momentum left which goes into the formation of a disk around the young star. Initially the disk is still embedded in an envelope of material from the core that has not yet been accreted onto the disk or star. This envelope feeds material onto the disk, as has been inferred from kinematics (see, e.g. Yen et al. 2015; van 't Hoff et al. 2018) and from the presence of shock-tracing molecular lines detected at the outer edge of the disk (see, e.g. Sakai et al. 2014). Over its lifetime this disk will have its angular momentum transported outward or carried away by disk winds, which drives the accretion flow of material onto the star until internal photoevaporation overcomes the stellar mass accretion and dissipates the disk (see, e.g. Alexander et al. 2014; Ercolano & Pascucci 2017). Mass accretion is likely a violent process, with instabilities in the disk resulting in episodic bursts of accretion (e.g. Zhu et al. 2009). Observationally accretion bursts have been linked to FU Orionis objects which undergo a sudden brightening in stellar luminosity (e.g. Herbig 1977; Hartmann & Kenyon 1996). The accretion onto the star also produces a jet which carves an outflow cavity in the envelope around the disk, which over a time period of $\sim 4 \times 10^5$ yrs disperses the envelope (e.g. Dunham et al. 2014).

Once the envelope has been dispersed the disk can be observed directly. From this point we refer to it as a *protoplanetary disk*. Historically it was thought that planet formation starts in this stage, but over recent years there is increasing evidence that planet formation already started at an early stage (see, e.g Tychoniec et al. 2020) and that protoplanetary disks host the planets and planetesimals that make up the beginnings of a planetary system.

1.2 Inside the disk: physics, chemistry and evolution

1.2.1 Disk (viscous) evolution

At its core a protoplanetary disk is an accretion disk. How the disk evolves therefore depends on the physics that drive the flow of material through the disk and onto the star. As the gas orbiting the star has some amount of angular momentum which has to be conserved, there needs to be a process which can either redistribute or remove angular momentum from the disk in order to drive the stellar mass accretion. There have been two processes proposed that fit this criterion: viscous stresses and magnetohydrodynamical (MHD) disk winds. Which of these processes is the dominant driver of disk evolution remains a topic of active research, as it provides information on the conditions inside the disk. For example, viscous evolution requires the disk to

be turbulent, which is not required for a disk-wind driven evolution. It is important to note that these two processes are not mutually exclusive: they can be operating at the same time (see, e.g. Suzuki & Inutsuka 2009; Bai & Stone 2013; Gressel et al. 2015; Béthune et al. 2017; Bai 2017).

Historically, it has commonly been assumed that protoplanetary disks evolve viscously. In the classical approach, where the disk is assumed to be a vertically thin axisymmetric sheet of viscous fluid, a shear causes the inner parts of the disk to lose angular moment to the outer parts of the disk (see, e.g. Lynden-Bell & Pringle 1974; Pringle 1981; Hartmann et al. 1998). This process causes the outermost part of the disk, which makes up only a small fraction of the mass, to expand outward and carry away the angular momentum. The bulk of the mass in the inner disk is instead forced inward where it is accreted onto the star.

Due to the uncertainties in what constitutes the viscosity it is common practice to describe the effects of viscous evolution using an "effective viscosity" also commonly known as the $\alpha-$disk prescription introduced by Shakura & Sunyaev (1973) for accretion disks around black holes. The advantage of this approach is that it describes the evolution of the disk using a single dimensionless parameter α. It should be kept in mind however that implicitly it is assumed here that α is constant with radius and in time, neither of which are guaranteed for the physical processes that constitute the effective viscosity.

What physical process actually makes up this viscosity is still a matter of debate. The molecular viscosity of the gas is too low; a back-of-the-envelope calculation results in a viscous timescale of $\sim 10^{13}$ yr, which is over six orders of magnitude longer than the expected lifespan of protoplanetary disks (see, e.g. Armitage 2019). An alternative proposed by Shakura & Sunyaev (1973) is that turbulence rather than molecular viscosity transports the angular momentum. A rigorous derivation by Balbus & Papaloizou (1999) showed that magnetohydrodynamical turbulence could in principle locally transport angular momentum (see also Balbus & Hawley 1991, 1998). Attempts at measuring turbulence in protoplanetary disks have either found no evidence (HD163296, MWC 480, V4046 Sgr; Flaherty et al. 2015, 2017, 2020) or measured low, subsonic turbulent velocities (TW Hya, DM Tau; Teague et al. 2016; Flaherty et al. 2020).

Viscous stresses are an internal way of redistributing the angular momentum, but it is also possible to do so using external processes. Most important here is the torque exerted by a MHD disk wind on the surface of the disks (see, e.g. Königl & Salmeron 2011; Frank et al. 2014). In the presence of a polodial vertical magnetic field, a disk wind can be launched from the disk surface. Angular momentum is transferred from the disk to the launched material as it is accelerated by the wind, causing the material remaining in the disk to move towards the central star (see, e.g, Blandford & Payne 1982 or Turner et al. 2014 for a review). Theoretical calculations show that these disk winds can remove some or all of the angular momentum required to drive the stellar accretion (see, e.g. Ferreira et al. 2006; Béthune et al. 2017; Zhu & Stone 2018). Observational evidence of this angular momentum removal has proven difficult, as direct observations of disk winds focus on the inner part of the disk (see, e.g. Pontoppidan et al. 2011; Bjerkeli et al. 2016; Tabone et al. 2017, 2020; de Valon et al. 2020).

With direct observations of both turbulence and disk winds proven difficult, another way of studying the physical processes that drive disk evolution is by examining how

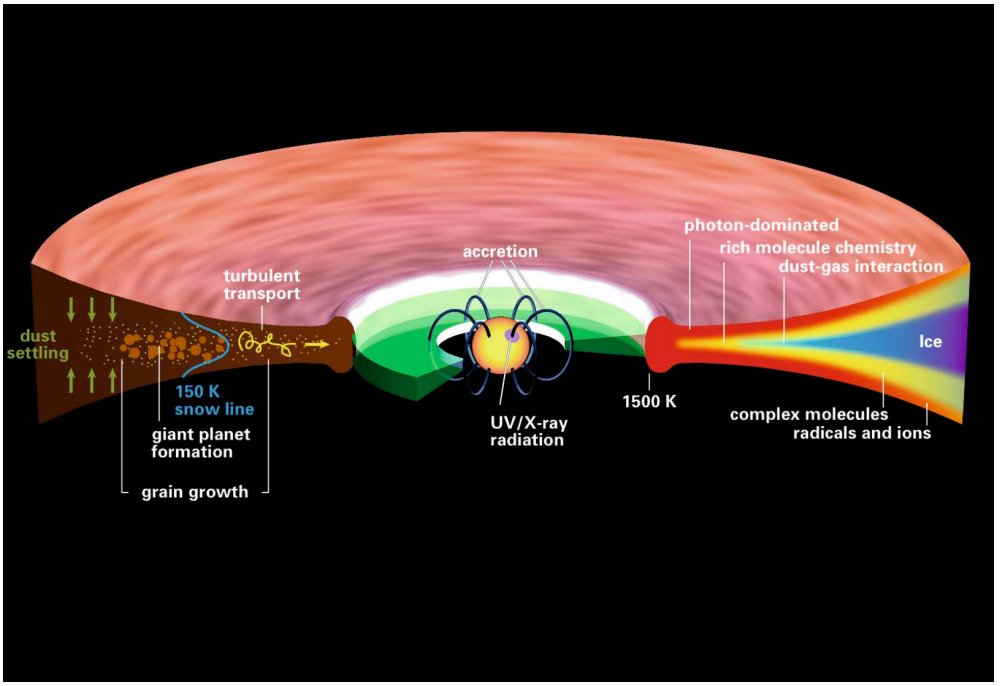

Figure 1.1: Schematic overview of a protoplanetary disk, showing on the left the processes relevant of the evolution of the dust (see also Section 1.2.3). On the right it shows how the chemistry changes from the surface to the midplane of the disk (see also Section 1.2.4). credits: Henning & Semenov (2013)

the disk structure, in particular its radius, reacts to the removal or redistribution of angular momentum. A viscously evolving disk should grow over time as the outer part of the disk expands outward, whereas a for a disk-wind driven evolution this is not the case (see, e.g. Lynden-Bell & Pringle 1974; Hartmann et al. 1998). This will be discussed in more detail in Chapter 4.

1.2.2 Disk structure

It is often assumed that the surface density of a protoplanetary disk follows a powerlaw that at larger radii tapers off exponentially (see, e.g. Hughes et al. 2008; Andrews et al. 2011). This surface density profile is a self-similar solution of a viscously evolving disk, assuming that the viscosity ν varies radially as a powerlaw $\nu \propto R^{\gamma}$ (see, e.g. Hartmann et al. 1998):

$$\Sigma_{\rm gas}(R) = \frac{(2-\gamma)\, M_{\rm disk}}{2\pi R_{\rm c}^2} \left(\frac{R}{R_{\rm c}}\right)^{-\gamma} \exp\left[-\left(\frac{R}{R_{\rm c}}\right)^{2-\gamma}\right]. \tag{1.1}$$

Here $M_{\rm disk}$ is the total disk mass and the characteristic radius $R_{\rm c}$ defines where the surface density profile transitions from a powerlaw to its exponential taper.

In addition to its link to viscous evolution this surface density profile also provides a natural explanation for the fact that observations show that gas line emission, in

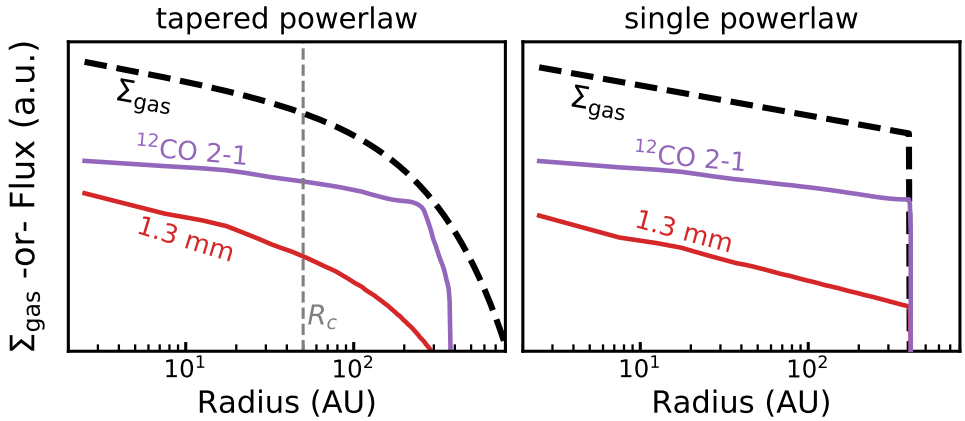

Figure 1.2: Two examples of surface density profiles (black dashed lines) and the corresponding ^{12}CO $J = 2 - 1$ line and 1.3 millimeter continuum radial intensity profiles, shown by the purple and red lines, respectively. The optically thin dust emission follows the surface density, while the optically thick CO emission decreases with the much shallower slope of the temperature profile. For the tapered powerlaw shown on the left the dust emission drops off rapidly at large radii while the CO is approximately at the same brightness.

particular of CO rotational lines, extends further out than continuum emission of the dust, a phenomenon that cannot be explained with only a powerlaw for both the gas and the dust (see, e.g. Panić et al. 2008). The CO emission is optically thick and can be easily detected to far out in the exponential taper of the surface density, down to column densities of $\sim 10^{15}$ cm^{-2}. The continuum emission is predominantly optically thin and therefore falls off rapidly once the surface density starts to decrease exponentially (see Figure 1.2 and e.g. Hughes et al. 2008).

Despite its common usage, it is still not clear how well this profile represents the true radial distribution of the gas, as determining the gas surface density from observations is challenging (see, e.g. Williams & McPartland 2016; Miotello et al. 2018). As an example, there is evidence that the gas profile in the outer disk falls of faster than a exponential taper (see Dullemond et al. 2020). On top of the uncertainties in its general shape it has also become clear that the gas density structure is not smooth. Clear examples are the so-called "transition disks" that show a clear inner cavity in both gas and dust (see, e.g. van der Marel et al. 2016a; Pinilla et al. 2018). High resolution observations at millimeter wavelengths have also shown a wide variation of substructures in the form of asymmetries, rings and dips (see, e.g. van der Marel et al. 2013; ALMA Partnership et al. 2015; Andrews et al. 2016; van Terwisga et al. 2018; Andrews et al. 2018a). Figure 1.4 shows a collage of protoplanetary disks observed at high resolution as part of the ALMA large program Disk Substructures at High Angular Resolution Project (DSHARP; Andrews et al. 2018a and accompanying publications). Most of these features are traced using continuum emission of the dust and therefore do not directly imply variations in the gas density. However, for some of these features a counterpart in the gas has also been revealed using deviations from Keplerian velocity (see, e.g. Teague et al. 2018, 2019; Rosotti et al. 2020).

The vertical structure of the gas is set by the condition that it is in hydrostatic

equilibrium, where gas pressure balances out the downward gravity exerted by the central star. Under the assumption that the disk is vertically isothermal the gas density follows a Gaussian distribution with a scale height $h \equiv c_s(T)/\Omega_K$, where $c_s(T)$ is the sound speed and Ω_K is the Keplerian orbital frequency (see, e.g. Chiang & Goldreich 1997; D'Alessio et al. 1998). Being vertically isothermal is a bit of an oversimplification. In truth the vertical temperature gradient requires the gas density to deviate slightly from a Gaussian to remain in hydrostatic equilibrium (see e.g. Armitage 2019). To explain the flat infrared spectra of T-Tauri stars, Kenyon & Hartmann (1987) proposed that disks are flared, where the height of the disk increases super-linearly with radius (see also Dullemond & Dominik 2005). Scattered light observations that trace the small grains at the disk surface show that most disks are indeed flared (see, e.g. Pantin et al. 2005; van Boekel et al. 2017; Avenhaus et al. 2018). These observations also reveal rings and gaps, suggesting that, analogous to the surface density, the scale height has radial variations (see, e.g. de Boer et al. 2016).

1.2.3 Dust evolution

For planets to form in protoplanetary disks, dust grains have to grow approximately thirteen orders from the micron sized grains found in the interstellar medium (see, e.g. Beckwith & Sargent 1991). Luckily, in the more dense environment found in protoplanetary disks these grains can grow efficiently through sticking, as shown in both theoretical calculations (see, e.g. Wada et al. 2008; Paszun & Dominik 2009; Krijt & Kama 2014; Krijt et al. 2015; Birnstiel et al. 2010, 2012) and experimental research (see, e.g. Blum & Wurm 2008; Güttler et al. 2010; Kothe et al. 2010; Weidling et al. 2012; Blum et al. 2014). The evidence for this growth can be seen in the detection of millimeter-sized and even centimeter-sized particles in protoplanetary disks (see, e.g. Rodmann et al. 2006; Ricci et al. 2010). Observations also indicate that grain growth occurs rapidly, with grains of millimeter sizes already present after $\sim 10^5$ yr (e.g. Harsono et al. 2018).

Grain growth is limited by two processes: fragmentation and radial drift. As the grains grow the relative speed at which they collide gets larger (see, e.g. Brauer et al. 2008) increasing the likelihood that these interactions lead to bouncing or fragmentation instead of growth. The exact threshold between growth and fragmentation, called the *fragmentation velocity*, depends on the composition of the grain and its surface. Experiments with silicate grains by Blum & Wurm (2008) show a fragmentation velocity of 1 m s^{-1}. The presence of an icy mantle is expected to increase the fragmentation velocity to ~ 10 m s^{-1} (Wada et al. 2008; Gundlach et al. 2011, but see also Gärtner et al. 2017), allowing grains to efficiently grow to centimeter sizes (Brauer et al. 2008; Windmark et al. 2012). Due to the higher velocities and densities, fragmentation sets the limit for grain growth in the inner disk. Further out the maximum attainable grain size is set by radial drift (see also Birnstiel et al. 2015).

As dust grains grow they start to experience more gas drag, causing them to decouple from the gas. The gas in orbit around the star is partially supported by the inward pressure gradient in the disk, causing it to move at sub-Keplerian velocities. The grains are not similarly supported and therefore move at Keplerian velocities, causing them to experience a "headwind" due to the slower moving gas. This interaction with the gas causes the grains to lose angular momentum, causing them to drift inward (see, e.g. Weidenschilling 1977; Takeuchi & Lin 2002). How quickly grains

drift inward depends strongly on the size and mass of the grains and on the density of the surrounding gas. The effect of gas drag on grains can be quantified by their Stokes number, sometimes also referred to as the dimensionless stopping time. The Stokes number compares the time required for the gas drag to stop the particle to the orbital time of said particle. Very small grains, or those that are very porous, have a Stokes number much smaller than one. They are dragged along by the gas and will not drift inward. At the opposite end of the scale, massive boulders that are tens of meters across have a Stokes number much larger than one. For them the angular momentum transfer to the gas is negligible: they simply plough through the gas. In between lie the grains of $\sim$ 0.1 mm - 1 m that have a Stokes number of approximately one, depending on their porosity and the properties of the surrounding gas. These grains experience the most gas drag and rapidly drift inward.

The physics behind radial drift can also provide an explanation for the rings seen in continuum emission at millimeter wavelengths. The gas drag causes dust grains move to where the gas pressure has a maximum, which in a smooth disk is at the position of the central star. However, a local overdensity in the gas will result in a local pressure maximum that can trap drifting dust grains (see, e.g. Whipple 1972; Pinilla et al. 2012). These local gas overdensities are commonly attributed to the presence of a planet in the disk, but other mechanisms such as dead zones have also been proposed (see e.g. Lyra et al. 2009).

Interactions with the gas also change the vertical distribution of the larger dust grains. As discussed in Section 1.2.2, the gas is vertically supported by a vertical pressure gradient which counteracts the vertical component of the stellar gravity. The decoupled larger dust grains are not similarly supported and instead are accelerated until there is enough gas drag to counteract the gravitational force. This *vertical settling* leads to a segregation of dust grains based on their size, with the larger grains being confined to the midplane of the disk (see, e.g. Dubrulle et al. 1995; Dullemond & Dominik 2004, 2005; Mulders & Dominik 2012; Riols & Lesur 2018). Vertical turbulence of the gas in principle counteracts dust settling by lifting grains back up, but it can only do so efficiently for the small grains that are well coupled to the gas (see, e.g. Fromang & Papaloizou 2006).

1.2.4 Chemistry in protoplanetary disks

Conditions in protoplanetary disks are diverse, spreading over a wide range of densities ($10^4 - 10^{12}$ cm^{-3}), temperatures (10-1000 K) and radiation fields, from strongly irradiated with X-ray and ultraviolet at the surface to completely dark in the disk midplane. This diverse environment leads to a diverse chemistry: photodissociation and photoionization, ion-neutral reactions, neutral-neutral reactions and gas-grain surface reactions. The chemistry in turn also affects its environment, as it sets the gas temperature through the changing heating-cooling balance, changes the level of ionization and it ultimately sets the composition of the material that goes into forming planets and their atmosphere.

The remaining chapters in this thesis make extensive use of rotational line emission of CO, emitted in the sub-millimeter, as tracer of the physical structure of the outer disk. As such, the chemistry that will be discussed here focuses on CO chemistry. In the outer disk the temperatures are low (10-100 K) and the chemistry is kick-started by high energy radiation and cosmic rays that are able to ionize various species (see,

e.g. Aikawa et al. 1997; van Dishoeck et al. 2006; Walsh et al. 2012). Reactions between these ions and neutral species are mostly barrierless, and thus efficient even at low temperatures, leading to a rapid ion-molecule chemistry (see e.g. Herbst & Klemperer 1973; Woodall et al. 2007). Freeze-out of molecules is another process that becomes important at the low temperatures found in the outer disk. The temperature at which a molecule freezes out onto the grains changes from molecule to molecule and depends on the gas temperature, resulting in temperature dependent variations in the composition of the gas (see, e.g. Öberg et al. 2011; Helling et al. 2014; Eistrup et al. 2016, 2018). Water freezes out at temperatures below ~ 150 K, meaning that beyond the inner few AU all available water is frozen out. The radius where a molecule transitions from predominantly gas phase to frozen out is defined as its iceline. For CO freeze out occurs at a lower temperature ($\sim 15 - 30$ K) and the CO iceline lies therefore further out, at several tens of AU (see e.g. Qi et al. 2013, 2015, 2019; Facchini et al. 2017; van 't Hoff et al. 2017; Zhang et al. 2017). Icelines of dominant carbon and oxygen carriers like H_2O, CO_2 and CO are thought to play an important role in the formation of planets. As discussed in Section 1.2.3, the expected increased stickiness of ice covered grains increases the efficiency of grain growth. Furthermore, Stevenson & Lunine (1988) suggested that water vapor released by ice grains that crossed the water iceline should diffuse back over the snowline and freeze out again, thus locally increasing the density of solids (see also Ciesla & Cuzzi 2006).

Vertically the disk can be divided into three chemically different zones (see Figure 1.3 or e.g. Aikawa et al. 2002; Bergin et al. 2007). High up in the disk, in what we will refer to as the *disk surface layer*, ultraviolet photons from the star can easily ionize and photodissociate molecules. As a result this layer is predominantly populated by neutral or ionized atomic species. The exact composition of this layer depends strongly on the color and strength of the ultraviolet radiation field, as photodissociation is different for different molecules and is sensitive to the shape of the radiation field (see, e.g. Heays et al. 2017). The first molecules that can survive in this layer are H_2, CO and N_2. Photodissociation of these molecules occurs through narrow lines in the far-ultraviolet ($912 - 1200$ Å), thus limiting the number of ultraviolet photons that are capable of photodissociating them. This process is referred to as self-shielding and allows these molecules to survive in the gas as soon as they have build up a sufficient column ($\sim 10^{15}$ cm^{-2} in the case of CO, see van Dishoeck & Black 1988). Note here that the dependence of self-shielding on discrete wavelengths results in isotope-selective photodissociation, This leads to less abundant isotopologues like $C^{18}O$ and $C^{17}O$ being destroyed by ultraviolet photons much deeper into the disk (see, e.g., Visser et al. 2009; Miotello et al. 2014).

Below the disk surface layer lies the *warm molecular layer* ($T_{\rm gas} \approx 30-70$ K). Here extinction due to e.g. small grains has reduced the ultraviolet radiation field enough that most molecules are no longer being photodissociated, while temperatures are still high enough that most molecules have not frozen out yet. This layer is of a particular interest for observers as most of the detected molecular line emission originates from this layer. In the outer disk H_2O and CO_2 are frozen out in this layer and CO is thought to be the dominant gas-phase carbon carrier. However, recent observations reveal that disks have overall low CO isotopolog line fluxes (see, e.g., Favre et al. 2013; Ansdell et al. 2016; Cleeves et al. 2016; Miotello et al. 2017; Long et al. 2017), and therefore draw into question whether CO is the main carbon carrier in this layer (see also Yu et al. 2017; Molyarova et al. 2017 for discussion).

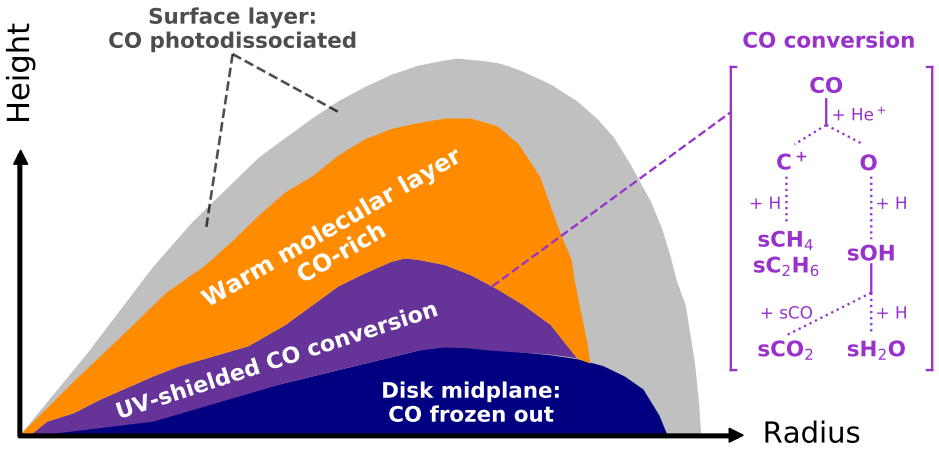

Figure 1.3: 2D sketch of the dominant chemistry affecting CO in different regions of a protoplanetary disk. On the right are the dominant paths through which CO can be converted in the UV-shielded region of the disk (adapted from Figure 2 in Bosman et al. 2018). Molecules frozen out on grains are denoted with an s in front. Note that non-thermal desorption provides a small amount of gas-phase CO in the midplane which can also be converted (see, e.g., Chaparro Molano & Kamp 2012; Helling et al. 2014).

As we move closer to the *disk midplane* the temperature decreases, resulting in the freeze-out of most molecules onto the grains. The previously discussed iceline of a molecule is therefore part of a larger "ice-surface" that marks the transition from gas-phase to solid state in both the radial and vertical direction. This layer is completely shielded from stellar and interstellar ultraviolet photons and X-rays. Instead, gas-phase chemistry is driven by cosmic-ray particles. These high energy particles can collide with molecular hydrogen and ionize it, producing a high energy electron. The H_2^+ can react with another H_2 to produce H_3^+ which starts the ion-molecule chemistry. The high energy electron will collide and excite multiple H_2, which upon de-exciting will produce secondary ultraviolet photons. Similar to higher up in the disk this weak ultraviolet field can dissociate molecules and produce radicals that can partake in chemical reactions. In this environment gas phase CO can be broken apart by He^+ into C^+ and O. The carbon will go into hydrocarbons like CH_4 and C_2H_6 which freeze out onto the grains. The oxygen that is produced also freezes out and hydrogenates to form H_2O or it reacts with the frozen out CO to form CO_2 (see, e.g. Figure 1.3 here or Figure 2 in Bosman et al. 2018). On the grains simple molecules like CO can also be hydrogenated to form more complex molecules like CH_3OH (see, e.g. Aikawa et al. 1997; Watanabe & Kouchi 2002; Cuppen et al. 2009; Bosman et al. 2018; Schwarz et al. 2018).

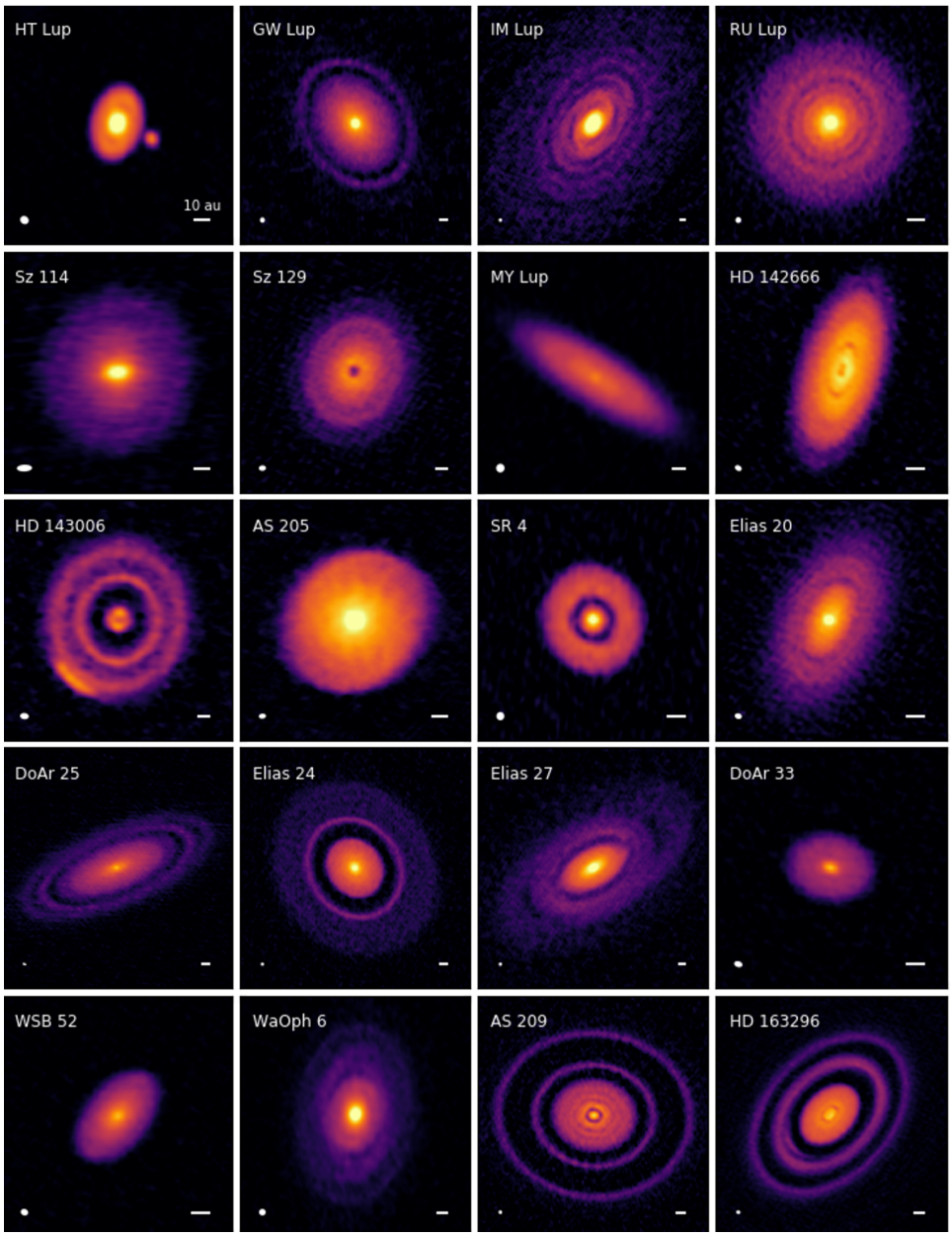

Figure 1.4: Image gallery of high resolution ALMA continuum observations of 25 bright disks (DSHARP large program; Andrews et al. 2018a). These images reveal a wide range of substructures in the dust. Colors show the intensity of the continuum, using an asinh stretch to reduce the dynamic range and accentuate fainter details. Beam sizes and 10 AU scalebars are shown in the lower left and right corners of each panel, respectively. Note that seven of these sources (HT Lup, GW Lup, IM Lup, RU Lup, Sz 114, Sz 129 and MY Lup) lie in the Lupus star-forming region, all of them among the top $\sim 17\%$ brightest disks found in Lupus.

1.3 Millimeter observations of protoplanetary disks: the ALMA era

If weighted by mass, most of the material in the disk resides in cold ($\sim 20 - 50$ K) molecular gas. This gas emits predominately through rotational line emission at millimeter wavelengths, as the rotational levels of most molecules can be easily excited at these temperatures. The Atacama Large Millimeter/sub-millimeter Array (ALMA) is the preeminent facility for observing protoplanetary disks at millimeter wavelengths, having both the sensitivity needed to detect the faint molecular emission and the sub-arcsecond resolution required to resolve the disk down to a few AU for typical distances to nearby star-forming regions. ALMA has allowed us to study individual objects at high resolution, revealing substructures in the dust in seemingly almost every disks examined in this way (see Figure 1.4 and e.g. ALMA Partnership et al. 2015; Andrews et al. 2016; Andrews et al. 2018a; Long et al. 2019).

Along a different axis, ALMA has allowed for large surveys covering all protoplanetary disks in an entire star forming region to be observed with short ~ 1 minute snap shots at sub-arcsecond resolution (e.g., Taurus, Ward-Duong et al. 2018; Long et al. 2018, 2019; Chamaeleon I, Pascucci et al. 2016; Long et al. 2017; σ-Ori Ansdell et al. 2017; Upper Sco, Barenfeld et al. 2016, 2017; Corona Australis, Cazzoletti et al. 2019; and Ophiuchus, Cox et al. 2017; Cieza et al. 2019; Williams et al. 2019). This has allowed us to study the disk population as a whole, which has shown that the "typical" protoplanetary disk is very different in size and mass from the large and bright individual disks studied previously.

Of particular interest for this thesis is the ALMA survey of the Lupus star-forming region (Ansdell et al. 2016; Ansdell et al. 2018). This program observed all 95 disk candidates in the region in ALMA Band 7 (~ 890 μm at $\sim 0\farcs3$ resolution, covering ^{13}CO $J = 3 - 2$, C^{18}O $J = 3 - 2$ and CN $N = 3 - 2$) and Band 6 (~ 1.3 mm at $\sim 0\farcs25$ resolution, covering ^{12}CO $J = 2 - 1$ ^{13}CO $J = 2 - 1$ and C^{18}O $J = 2 - 1$). Of the 95 disk candidates, $\sim 75\%$ are detected in the continuum. For the gas detection rates are much lower, $\sim 50\%$ for ^{12}CO, $\sim 21 - 40\%$ for ^{13}CO and $8 - 12\%$ for C^{18}O. A complementary survey targeted most of these sources with the X-Shooter instrument (Vernet et al. 2011) on the Very Large Telescope (Alcalá et al. 2014, 2017). Combined, these surveys provide a wealth of data on the properties of disks and how these depend on their host star (see, e.g. Manara et al. 2017). Figure 1.5 and 1.6 show overviews of all disks found in the Lupus star-forming region (see also Ansdell et al. 2016; Ansdell et al. 2018). In the next part we focus on two properties: How large is a typical protoplanetary disk? And how much material, i.e. gas and dust, does it contain?

1.3.1 Measuring disk radii

The size of a protoplanetary disks is an important tool for studying the evolution of the gas and the dust in the disk. Do disks grow over time, indicating that they evolve viscously? How much have the larger grains drifted inward with respect to the gas and the small grains? To answer these questions, we need to measure a disk size from the observations and understand how it traces the underlying structure of the disk.

The size of the disk can be measured from the millimeter continuum emission, which shows how extended the millimeter-sized grains are distributed. The continuum emission is easy to detect, making it the most accessible measured disk size. The

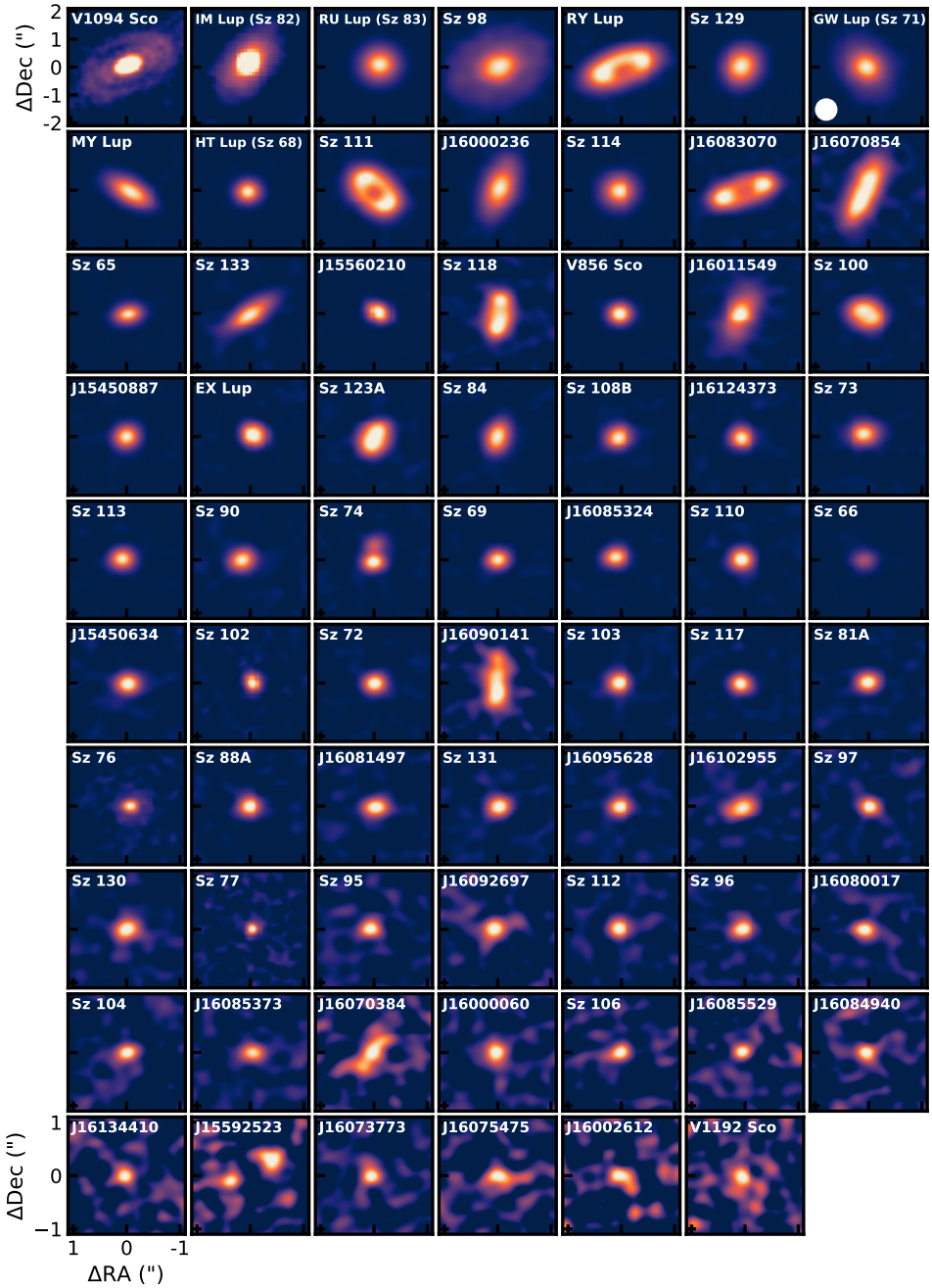

Figure 1.5: Group photo of the disk population in the Lupus star-forming region, located at a distance of $\sim$ 160 pc, showing the 890μm (Band 7) continuum images observed with ALMA (Ansdell et al. 2016). The images are $2\farcs2 \times 2\farcs2$ and are ordered by decreasing continuum flux. The color scale in each image runs from the peak flux to zero. V1094 Sco and IM Lup are shown in $4\farcs2 \times 4\farcs2$ images and their continuum fluxes in the center have been saturated by 70% to better reveal their faint outer disk.

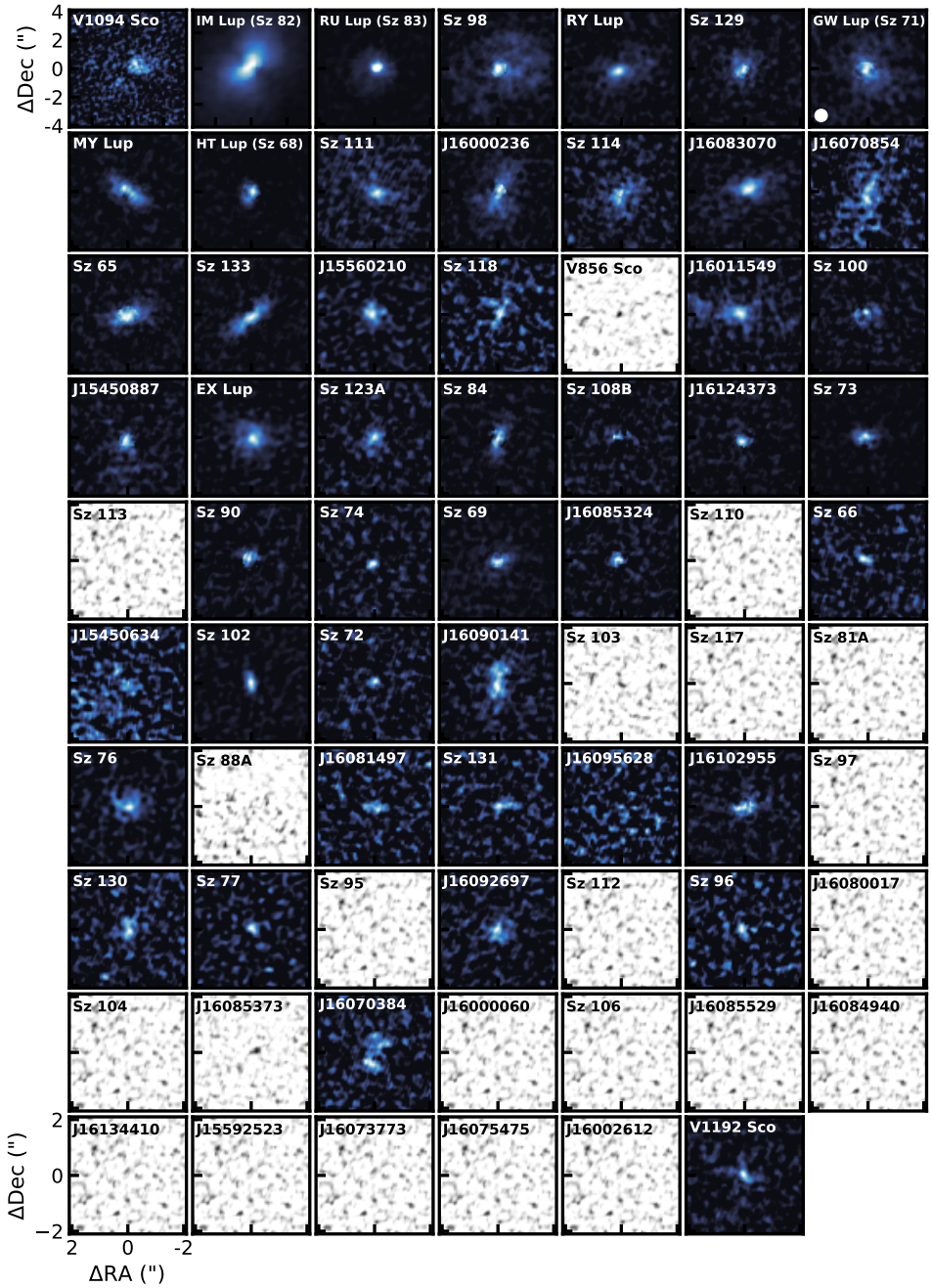

Figure 1.6: As Figure 1.5, but now showing the ^{12}CO $J = 2 - 1$ integrated intensity maps observed with ALMA Band 6. The disks are again ordered by decreasing continuum flux, but the sizes of images have been increased to $4\farcs2 \times 4\farcs2$ ($8\farcs2 \times 8\farcs2$ for V1094 Sco and IM Lup). The color scale in each image runs from the peak intensity to zero. Sources for which ^{12}CO $J = 2 - 1$ was not detected are shown in black and white.

measured dust disk size depends on the wavelength of the continuum emission, with disks becoming more compact at longer wavelengths, likely due to the larger grains having drifted inward more quickly than smaller grains (see, e.g. Tazzari et al. 2016; Tripathi et al. 2018). With the advent of ALMA disk surveys, there is now a large sample of disks for which the dust disk size has been measured (see, e.g. Andrews et al. 2013; Ansdell et al. 2016; Tazzari et al. 2017; Tripathi et al. 2017; Andrews et al. 2018b; Long et al. 2018; Tobin et al. 2020). Overall, it has been found that many protoplanetary disks are small in the dust: only $\sim 2\%$ show continuum emission beyond 200 AU (van Terwisga et al. 2018) and approximately 45% of disks remain unresolved at 0.2 arcsecond resolution, implying radii smaller than 25 AU. This could mean that the bulk of protoplanetary disks is small. However one should keep in mind that these dust disk sizes are measured from continuum emission emitted by millimeter-sized grains which likely have drifted inward (as discussed in Section 1.2.3). The availability of large samples of measured dust disk sizes have allowed us to look for correlations with other disk and stellar parameters (see, e.g. Tazzari et al. 2017; Tripathi et al. 2017; Andrews et al. 2018b; Rosotti et al. 2019a). These studies show that the dust disk size is directly correlated with the dust mass or total millimeter luminosity. This correlation can be reproduced by assuming that the dust is concentrated in optically thick rings that fill $\sim 30\%$ of the disk surface (Tripathi et al. 2017; Andrews et al. 2018b). If this is the case, the millimeter flux would be just a measure of the disk surface area. High resolution observations also show evidence towards a link between presence of rings and the measured dust disk size (see, e.g. Long et al. 2019).

Our understanding of the extent of the gas in protoplanetary disks is more limited compared to the dust. The bulk of the gas is made up by molecular hydrogen, which does not emit in the conditions found throughout most of the disk (this will be discussed in more detail in Section 1.3.2). The gas disk size is therefore measured from the extent of other molecules like CO and CN, whose bright line emission is often detected towards protoplanetary disks (for a non-exhaustive list, see, e.g. Piétu et al. 2005; Schaefer et al. 2009; Piétu et al. 2014; Guilloteau et al. 2014; Simon et al. 2017; Barenfeld et al. 2017; Ansdell et al. 2018). The challenge then lies with understanding what these indirect tracers tell about the underlying bulk distribution of the gas. Line emission from ^{12}CO is optically thick, making it bright and easier to detect out to large radii, but also making it more challenging to link the extent of the emission to how spread out the gas is. Using more optically thin isotopologs like ^{13}CO or C^{18}O would circumvent this, but detecting these lines further out in the disk requires deeper observations that are currently only available for a small number of sources. The CN molecule is a photodissociation tracer that is abundant high up in the disk. When observed at high spatial resolution with ALMA the emission is found to be ring shaped (see, e.g. Teague et al. 2016; van Terwisga et al. 2019). Models by Cazzoletti et al. (2018) show that the location of the ring depends on the radial distribution of the gas and the strength of the ultraviolet radiation field. Based on the same models van Terwisga et al. (2019) showed that the low CN fluxes observed towards many disks can only be explained with small gas disks.

Our understanding of gas disk sizes is still predominantly based on individual objects, most often bright disks around solar mass stars, as obtaining a large sample of measured gas disk sizes comparable to the dust disk sizes has proven difficult to be approved by time allocation committees. Recent ALMA disk surveys in most cases also covered ^{13}CO and C^{18}O, and in some cases ^{12}CO, but the 1 minute snapshots

proved too shallow to detect CO at high enough sensitivity to accurately measure the gas disk size.

Ansdell et al. (2018) targeted 95 disks in Lupus with ALMA, detecting ^{12}CO $J = 2 - 1$ in 48 sources ($\sim 51\%$) and was able to measure gas disk sizes for 22 ($\sim 23\%$) sources due to a low signal-to-noise (for more details, see Chapters 2 and 3). They find that gas disk sizes of these 22 disks are universally larger than their dust disk size by a factor of ~ 2 (see Figure 1.7). This could indicate that the millimeter grains have drifted inward, although in Chapters 2 and 3 it will become clear that due its larger optical thickness, the CO line emission will always extend further out than the optically thin dust emission (see also Figure 1.2). They find a tentative correlation between the gas disk size and the total continuum flux but no correlation with stellar mass. Barenfeld et al. (2017) was able to measure gas disk sizes for seven of the 21 disks in Upper Sco where they were able to detect ^{12}CO $J = 2 - 1$. For four of their sources the CO emission is more extended than the dust, although these observations suffer from a low signal-to-noise.

1.3.2 Measuring disk masses

The total mass of protoplanetary disks is a quantity of great interest, as it represents the reservoir of material available to form and grow planets. Measuring the disk mass has proven challenging (see, e.g. Bergin et al. 2019). Most of the disk mass resides in the gas, made up predominantly by molecular hydrogen (H_2), a light, symmetric molecule. The lack of a permanent electric dipole moment limits its rotational transitions to quadrupole transitions ($\Delta J = 2$). To produce significant H_2 emission the $J = 2$ level at $E/k_B = 549.2$ K has to be excited, which requires gas temperatures of at least 100 K (see, e.g. Thi et al. 2001; Carmona et al. 2011). As most of the gas in protoplanetary disks has a much lower temperature, H_2 emission does not trace the bulk of the mass (see, e.g. Pascucci et al. 2013). Even when excited the transitions of H_2 are weak and lie in the mid- and near-infrared where the continuum emission from the dust is also bright, making the detection of H_2 a challenge due to its low line/continuum ratio. Furthermore, the continuum becomes optically thick at these wavelengths very high up in the disk, effectively hiding the H_2 below. Measuring the disk mass thus requires an indirect tracer.

The most common indirect gas mass tracer is carbon monoxide (CO) and its optically thin isotopologues. After molecular hydrogen CO is the second most abundant molecule in the gas. The main isotopolog, ^{12}CO, is optically thick throughout most of the disk, requiring us to go to less abundant isotopologs like ^{13}CO, C^{18}O, C^{17}O and sometimes even ^{13}C^{17}O and ^{13}C^{18}O to measure the total amount of CO in the disk. Relating the total amount of CO to the gas mass requires knowledge of the CO abundance with respect to molecular hydrogen. For this reason, the chemistry of CO in protoplanetary disks has been well studied (see, e.g., van Zadelhoff et al. 2001; Yu et al. 2017; Bosman et al. 2018; Schwarz et al. 2018). Using models that include photodissociation and freeze-out, the dominant processes that affect the CO abundance, the disk gas mass can be derived from observations of ^{13}CO and C^{18}O (see, e.g. Miotello et al. 2014; Miotello et al. 2016; Williams & Best 2014,). Disk surveys carried out with ALMA have used this method to measure gas masses for a large number of protoplanetary disks, although this number is still low compared to the number of measured dust masses (see, e.g. Ansdell et al. 2016; Ansdell et al. 2018;

Figure 1.7: A collage of 10 disks in $2\farcs2 \times 2\farcs2$ stamps from the Lupus survey, showing the ^{12}CO $J = 2 - 1$ emission in blue on one side of the disk and the 890μm continuum emission in purple on the other side of the disk. The blue contours show a $S/N = 2$ for the CO emission. The purple contours show a $S/N = 3$ for the continuum emission. Note that Sz 76, Sz 130 and V1192 Sco remain unresolved in the continuum. The CO emission is found to be more extended than the continuum emission, but the low S/N of the CO emission also highlights the limitations of the ~ 1 minute snapshots of disk surveys.

Long et al. 2017; Miotello et al. 2017,). These CO-based gas masses are found to be low, with most disks having a gas-to-dust mass ratio $\Delta_{\rm gd} \sim 1 - 10$, much lower than the ISM value ($\Delta_{\rm gd} \sim 100$). Whether this implies that disks are gas poor or that there exists a process that removes gas-phase CO that currently is not included in the analysis remains an open question, although as will be discussed below the second explanation seems to be favored.

Another promising gas mass tracer is hydrogen deuteride (HD). Being an isotopolog of H_2, HD has been shown to directly follow the distribution of H_2 (see Trapman et al. 2017). The asymmetry of HD gives rise to a small dipole moment and dipole transitions ($\Delta J = 1$). For a gas at a temperature of ~ 20 K it is much easier to excite the first rotational energy level of HD ($E/k_B = 128.5$ K) compared to exciting the second rotational energy level of H_2 ($E/k_B = 549.2$ K), resulting in significantly more emission from HD compared to H_2 in protoplanetary disks. Trapman et al. (2017) show that for low mass disks ($M_{\rm disk} \leq 10^{-3}$ $M_\odot$) the HD $J = 1 - 0$ line flux at 112 μm can be used to directly measure the gas mass to within a factor of two. For more massive disks the gas mass can be measured to within a factor of 3 by combining HD $J = 1 - 0$ with the HD $J = 2 - 1$ line flux at 56 μm or a similar tracer of the disk temperature structure.

The energetically lowest transition of HD at 112 μm lies in the far-infrared, where the atmospheric opacity requires going to space-based observatories. Using the PACS (Poglitsch et al. 2010a) instrument on the *Herschel Space Observatory* (Pilbratt et al. 2010a) HD $J = 1 - 0$ has been detected towards three disks, TW Hya, DM Tau and GM Aur, before the instrument was shut down (Bergin et al. 2013; McClure et al. 2016). Gas masses measured for these sources are higher compared to their CO-based gas masses, finding gas-to-dust mass ratios of $\Delta_{\rm gd} \approx 100$ (Bergin et al. 2013; McClure et al. 2016; Trapman et al. 2017). This has spurred the field to examine chemistry and physical processes that are currently not included in the models that can explain the low CO-based gas masses (see, e.g. chemistry Aikawa et al. 1997; Favre et al. 2013; Bergin et al. 2014; Yu et al. 2017; Schwarz et al. 2018; Bosman et al. 2018, physical processes Bergin et al. 2010; Bergin et al. 2016; Du et al. 2015; Kama et al. 2016b; Krijt et al. 2018 or a combination of the two: Krijt et al. 2020). With the current lack of an observatory capable of detecting HD in protoplanetary disks, we are unable to verify that the results of this small sample of three disks is representative for the full disk population.

Compared to the gas mass, the dust mass is more accessible. Under the assumption that the continuum emission emitted by the dust is optically thin at millimeter wavelengths, there is a simple conversion between the observed flux $F_{\rm mm}$ and the total amount of dust $M_{\rm dust}$ in the disk (see, e.g. Hildebrand 1983; Beckwith et al. 1990)

$$M_{\rm dust} = \frac{d^2}{\kappa_\nu B_\nu(T_{\rm dust})} F_{\rm mm}. \tag{1.2}$$

Here d is the distance to the source, κ_ν is the dust mass opacity, $B_\nu(T_{\rm dust})$ the Planck function at the temperature of the dust, commonly assumed to be $T_{\rm dust} = 20$ K. The conversion from flux to mass is not free from uncertainties. The assumption that the dust is optically thin may not be valid for all parts of the disk, especially if the dust is concentrated in ring-like structures (see, e.g. Dullemond et al. 2018). Another uncertainty is the dust mass opacity. The dust mass opacity depends on the composition of the grains which is not well known (see, e.g. Weingartner & Draine

2001; Draine 2006; Dullemond et al. 2018). A further ingredient that goes into the mass opacity is the grain size distribution, where multi-wavelength observations have put constraints (see, e.g. Tazzari et al. 2016). Finally, scattering at millimeter wavelengths can reduce the flux coming from optically thick regions of the disk, making them appear optically thin, thus leading to an underestimation of the dust mass. In simple models this process is often thought to be negligible, but recent results show that this might not always be case (e.g. Zhu et al. 2019).

To determine the total disk mass requires the ratio of gas to dust in the disk. As discussed previously, the gas-to-dust mass ratio ($\Delta_{\rm gd}$) is found to be approximately 100:1 in the ISM. In disks the ratio is expected to be higher, as the radial drift has caused the large grains to be accreted onto the star (see, e.g. Youdin & Chiang 2004). Furthermore, part of the initial dust mass reservoir has (presumably) been converted into planets or planetary embryos. On the other hand, gas dissipation processes, such as external photo-evaporation, will decrease the $\Delta_{\rm gd}$.

Using ALMA, surveys of multiple star-forming regions have been carried out, which have provided us with an inventory of disk dust masses of the full disk population. These surveys show that the bulk of the disk is less massive than previously thought, with a median disk dust mass of ~ 5 M$_\oplus$ for a 1-3 Myr old star-forming region, assuming a mass opacity of $\kappa_{1.3\rm mm} = 2.3$ cm^2 g^{-1} and a disk-averaged dust temperature of $T_{\rm dust} = 20$ K (see, e.g. Ansdell et al. 2016; Ansdell et al. 2018; Pascucci et al. 2016). This mass already has difficulty explaining the total amount of solids found in exoplanets, without even taking into account that the mass efficiency of planet formation is likely much less than one (see, e.g. Najita & Kenyon 2014; Manara et al. 2018). This discovery has been one of the main drivers for advocating that planet formation already starts in the earlier embedded phase, where disks are found to be more massive (see, e.g. Tychoniec et al. 2018, 2020; Tobin et al. 2020). The surveys also show that the median dust mass decreases with the age of the star-forming region, although recent surveys suggest that this is not a one-to-one correlation (Ansdell et al. 2017; Cazzoletti et al. 2019; Williams et al. 2019).

1.4 Modeling protoplanetary disks

Modeling the emission of protoplanetary disks provides a means of linking what is observed, e.g. the amount, extent and shape of continuum and line emission, to the underlying disk structure and composition. By solving the radiative transfer equation, the dust continuum emission can provide information on the disk dust structure, dust temperature and dust composition. Examples of such 2D/3D continuum radiative transfer codes are `RADMC3D` (Dullemond & Dominik 2004; Dullemond et al. 2012), `TORUS` (Harries et al. 2004; Harries 2014; Harries et al. 2019), `MCFOST` (Pinte et al. 2006), `MCMax` (Min et al. 2009), `Hyperion` (Robitaille 2011) and `POLARIS` (Reissl et al. 2016). Line emission can reveal details on the temperature, distribution and composition of the gas, depending on the molecule used for the analysis. Line radiative transfer codes such as `LIME` (Brinch & Hogerheijde 2010), `FLiTs` (Woitke et al. 2018), `RADlite` (Pontoppidan et al. 2009) and `POLARIS` (Brauer et al. 2017) use inputs such as gas temperature, molecular density and the radiation field to compute line excitation and line emission. In protoplanetary disks gas temperature, line excitation and the chemistry that set molecular abundances are interdependent properties. Several modeling codes have therefore been developed that combine the previously mentioned

modeling components into a self-consistent disk model. Examples include `DALI` (Bruderer et al. 2009, 2012; Bruderer 2013), `ProDiMo` (Woitke et al. 2009; Kamp et al. 2010; Thi et al. 2011)(and in extension the DIANA project; Woitke et al. 2016, 2019; Kamp et al. 2017), `RAC2D` (Du & Bergin 2014) and `ANDES` (Akimkin et al. 2013). In these models the dust temperature, gas temperature, chemistry and excitation are calculated self-consistently. In the interest of keeping computation time manageable these models make some simplifications, such as assuming a static, and often parametric, density structure, using a simpler chemical network focused on accurately reproducing the heating and cooling in the disk or making simplifying assumptions about the excitation and radiative transfer such as using an escape probability.

Broadly speaking there are two approaches for modeling, inverse modeling and forward modeling, which have complementary goals. In inverse modeling the aim is to characterize the disk structure, in terms of density, temperature and abundance, that best describes a given set of observations. Briefly, for a given disk model the previously discussed codes can be used to compute the expected emission, which is then compared to the observations, varying the disk parameters to minimize the residuals. To accurately measure formal uncertainties on the parameters that describe the disk structure, for example using a Monte-Carlo Markov Chain method (e.g. Foreman-Mackey et al. 2013), it is necessary to run tens or even hundreds of thousands of models. To make this computationally feasible the approach focuses on radiative transfer codes where running such a number of models is attainable (see, e.g. Andrews et al. 2011; Tazzari et al. 2017; Tazzari et al. 2018; Cieza et al. 2018), although there are also examples of inverse modeling using thermochemical codes (see, e.g. Kama et al. 2016b; Fedele et al. 2017; Woitke et al. 2019).

The alternative approach is forward modeling. In this approach the focus is on accurately portraying the physics and chemistry in protoplanetary disks. By varying the parameters that govern these processes one can inspect the resulting change in observables, such as the amount or distribution of emission. Forward modeling is aimed at characterizing trends between disk properties and observables. Examples include CO isotopolog line fluxes as tracer of disk gas mass (see, e.g. Williams & Best 2014; Miotello et al. 2014; Miotello et al. 2016), the link between CN emission and the size of the disk and far-ultraviolet radiation it is exposed to (Visser et al. 2018; Cazzoletti et al. 2018) and understanding mid-IR and far-IR water features observed in disks with *Spitzer* (Antonellini et al. 2015, 2016).

1.5 This thesis

Over recent years our understanding of protoplanetary disks has grown considerably. However there are still gaps in our knowledge of planet formation. The wide variety of exoplanets and planetary systems is no less than the diversity of the properties of protoplanetary disks they once inhabited. Furthermore, the fact that each star hosts at least one planet (see, e.g. Cassan et al. 2012; Suzuki et al. 2016) on average means the puzzle of planet formation must not only be solved for the previously studied bright, large disks but for the full protoplanetary disk population. The disk surveys with ALMA of entire star-forming regions (e.g. Lupus: Ansdell et al. 2016; Ansdell et al. 2018) have provided the first steps here. This thesis focuses on CO line observations from these surveys, in particular those from the Lupus disk survey. Thermochemical models are used to bridge the gap between observables, such the gas disk size measured

from CO, and the underlying bulk properties and distribution of the gas. Based on these observables, the thesis examines physical processes in protoplanetary disks, such as grain growth and radial drift of large dust grains and the viscous evolution of the gas.

Chapter II and III of this thesis look at the effects of radial drift and grain growth on the difference between observed gas and dust disk sizes. The fact that in observations the CO line emission extends further out than the dust continuum is (often solely) attributed to larger grains having radially drifted inward. As discussed previously, the difference in optical depth between the two tracers can produce a similar observational signature. Chapter II examines quantitatively the effects of dust evolution and optical depth on the observed gas-dust size differences. In Chapter III the lessons learned in the previous chapter are applied to the observed gas and dust disk sizes of protoplanetary disks in the Lupus star-forming region. For a sample of ten disks dust-based models without radial dust evolution are used to investigate whether dust evolution is required to reproduce the observations.

Chapter IV examines measured gas outer radii in the context of protoplanetary disks evolving viscously. In viscous evolution theory disks grow over time, an observable feature that distinguishes it from wind-driven disk evolution. This chapter investigates whether the measured gas outer radius is a suitable tracer for viscous spreading and compares models to observations in the Lupus and Upper Sco star forming region to determine if disks evolve viscously.

In chapters V and VI the focus shifts to the gas mass of protoplanetary disks. Chapter V examines the behavior of ^{13}CO and C^{18}O line fluxes of viscously evolving disks. It also investigates whether CO destruction at the disk midplane can reconcile the gas masses required to explain the observed stellar mass accretion rates with the low ^{13}CO and C^{18}O fluxes observed towards protoplanetary disks. In Chapter VI HD $J = 1 - 0$ upper limits obtained from archival *Herschel* observations are examined. Combined with an extensive grid of disks models these upper limits are used to place meaningful constraints on the gas masses of disks around Herbig Ae/Be stars.

The main conclusions of the thesis can be summarized as follows:

Chapter II: The gas disk size measured from models is not affected by dust evolution and traces the radius in the outer disk where the CO column density drops below 10^{15} cm^{-2} and CO becomes photodissociated. To accurately measure the gas outer radius requires a peak signal-to-noise greater than 10 for the ^{12}CO integrated velocity map. A measured gas disk size ($R_{\rm gas}$) that is more than four times as large as the dust disk size ($R_{\rm dust}$) is a clear sign that the disk has undergone grain growth and radial drift. Disks for which the difference in sizes is smaller require modeling of the CO emission to separate optical depth effects from the impact of dust evolution on gas and dust disk sizes.

Chapter III: Out of a sample of ten observed disks in the Lupus star-forming region, all with $R_{\rm gas}/R_{\rm dust} < 4$, five require dust evolution in addition to optical depth effects to explain both their dust structure and the observed gas disk size. For the other five disks the observed gas–dust size ratio can be explained without dust evolution, using only optical depth effects. An additional six disks from the same star-forming region are found to have significant, i.e. $S/N \geq 3$, CO 2-1 emission out beyond four times their dust outer radius. While low S/N prevents detailed analysis, it would be difficult to explain the observations of these six

disks without substantial dust evolution.

Chapter IV: Our models show that gas outer radii measured from CO emission are a suitable tracer of viscous expansion: the gas radius increases over time and does so faster if the disk is expanding at a faster rate. However, in the case of a low mass disk expanding rapidly, the gas outer radius measured from our models is found to instead decrease with time as a result of photodissociation in the outer disk. Our models also reveal that quantitatively linking the observed outer radii to viscous evolution is more difficult and can overestimate the amount of viscosity in the disk by up to an order of magnitude. Most observed gas outer radii of disks in Lupus are found to be consistent with viscously evolving disk models that start out small (≤ 10 AU) and evolve with a low viscosity.

Chapter V: For a viscously evolving disk the gas mass decreases over time, but the ^{13}CO and C^{18}O line fluxes of our models, used to trace the gas mass, instead increase over time as their optically thick emitting regions grow in size. Observed ^{13}CO and C^{18}O fluxes of the most massive ($M_{\rm disk} > 5 \times 10^{-3}$ M$_\odot$) disks in Lupus can be reproduced by our viscously evolving disk models. For lower mass disks the observed ^{13}CO and C^{18}O fluxes are up to an order of magnitude fainter compared to the models. CO conversion through cosmic-ray driven chemistry can potentially reconcile the difference for C^{18}O, but it cannot explain this difference for ^{13}CO as CO is predominantly destroyed below the ^{13}CO emitting region. To explain the observed ^{13}CO fluxes and C^{18}O upper limits in Lupus low mass ($M_{\rm dust} \leq 5 \times 10^{-5}$ M$_\odot$) disks either have to be significantly smaller than their more massive counterparts, or they must undergo efficient vertical mixing.

Chapter VI: The HD upper limits constrain the gas masses of nearly all disks to below 0.1 M$_\odot$, thus ruling out that these disks are currently gravitationally unstable. The strongest constraint is obtained for the disk around HD 163296, $M_{\rm gas} \leq 0.07\,$M$_\odot$, which combined with the dust mass suggests that the disk has a global gas-to-dust mass ratio below 100. The HD-based gas mass upper limit lies at the low end of gas masses estimated based on CO isotopologues, suggesting that CO is underabundant by at most a factor of a few. The gas mass upper limits of HD 163296 and HD 100546, two disks that host several massive candidate protoplanets, suggest disk-to-planet mass conversion efficiencies of $\sim 10 - 40\%$ based on current values.

Gas outer radii measured from ^{12}CO emission have a well understood link to the underlying extent of the gas and are therefore a robust measure of the size of the gas disk. As an observable, the gas outer radius is a valuable tool to study radial drift of large grains when combined with the outer radius of the dust. It can also show what physics drive disk evolution if paired with the age of the disk. However, this thesis has shown that modeling is required to accurately interpret observed gas outer radii. Explaining the faint CO isotopolog line fluxes that have been observed likely requires a combination of processes put forward in the literature. With HD remaining our most direct link to the gas mass of protoplanetary disks, a renewed access to the HD rotational lines in the far-infrared would greatly increase our understanding of this elusive quantity.

1.5.1 Future outlook

ALMA has provided some extraordinary and far-reaching results, but, fortunately for us, it is only getting started revealing the intricate inner workings of protoplanetary disks. One area that has remained relatively unexplored is the distribution and composition of the gas in disks. Despite outweighing the dust in disks by a factor ~ 100, after 8 years of ALMA there have been very few deep gas observations in disks compared to the detailed and deep studies of the dust. The recently observed MAPS ALMA (PI: Öberg) large program will provide deep gas observations of a wide range at high ($\sim 0\farcs1$) resolution of five disks. These observations will provide a wealth of information of the gas in disks, but placing them in context of the disk population as a whole requires a revisit of the disk surveys of several star-forming regions carried out with ALMA. These previous disk surveys have been very successful, but they were tailored towards observing the dust continuum and, in hindsight, were too shallow to robustly detect and study the gas emission for the full disk population. One of main next goals of ALMA should therefore be disk surveys that focuses on the gas. As it stands, we know only little of the structure of the gas of disks with low dust mass. Are they as small as their compact dust emission suggest or are we seeing the effect of efficient inward drift of millimeter-sized grains? Using a setup similar to previous surveys but going for 10-30 minutes per source covering CO and its main isotopologs would give us a wealth of information on the properties of the gas of a typical protoplanetary disk.

Currently one of our largest blind spots for in terms of protoplanetary disk research is the lack of a facility capable of observing in the far-infrared, after the *Herschel Space Observatory* shut down. This wavelength range contains the HD rotational lines that are key for measuring disk gas masses and covers several H_2O lines used to detect the presence of cold water in protoplanetary disks. With the recent cancellation of the HIRMES instrument development in April 2020, the future of this wavelength range now lies with the proposed *Space Infrared Telescope for Cosmology and Astrophysics* (SPICA), hopefully to be approved in summer of 2021, and the *Origin Space Telescope* (OST). Both missions will likely not fly before the mid 2030s, but they will be worth the wait.

The *James Webb Space Telescope* (JWST) is closer over the horizon. With its near- and mid-infrared instruments it will focus mostly on the inner few AU of the disk. However, this inner disk and the outer disk are linked. We cannot properly interpret what we see in the outer disk without understanding the structure of the inner disk. For example, if CO is removed from the outer disk through freeze-out and transformation and subsequently transported inward over the CO_2 and H_2O icelines, the enhancement in volatile carbon in the inner disk should be measurable with JWST.

The low average dust mass of protoplanetary disks means that planet formation needs to start already while the disk is still embedded in an envelope. While observations show that the material is there at an early age, we also need to find out if the conditions are favorable for planet formation. For example, can the dust grow fast enough into planetary embryos in the few 10^5 yrs that the disk is embedded? This requires shifting our modeling from building planets in protoplanetary disks to doing so in younger disks. To support this modeling effort we also need observations to uncover the conditions inside these disks. There is already an accepted ALMA large program (PI: Ohashi) to observe 7 Class 0 and 10 Class I disks at AU scale resolution to look for substructure in these young objects. To what extent these substructures are already present will inform us on just how early planets have started to form.

The wealth of new and upcoming observations will bring forth changes and new challenges for our models of protoplanetary disks. For example, observations show that substructures are ubiquitous at least in bright disks, but a large number of models are still run using a smooth density profile Furthermore, it has become increasingly clear that some observations cannot be explained using our static, axisymmetric disk models. A prime example is the riddle of the low CO isotopolog line fluxes, which, as will be discussed later in this thesis, are very difficult to explain using a static disk. It was recently shown that the solution might lie in combining the effects of chemistry with the evolution of the dust (Krijt et al. 2020). This typifies the next major step in disk modeling, where we examine the interplay between the evolution of the dust, the radial and vertical movements of the gas and the chemistry both in the gas as well as on the dust grains. This in itself is not without its challenges, as the complexity of the model increases rapidly with the number of components that are included. We should therefore keep in mind that the goal is to understand the effect of the physics and chemistry that we include and how observations can show us their relative importance. It is tempting to include everything in single model, but remember that we are here to understand what we see, not simply reproduce it.